ESMO GOOD SCIENCE BETTER MEDICINE BEST PRACTICE

Annals of Oncology 28: 2827–2835, 2017
doi:10.1093/annonc/mdx489
Published online 11 September 2017

ORIGINAL ARTICLE

An exploratory, open-label, randomized, multicenter study to investigate the pharmacodynamics of a glycoengineered antibody (imgatuzumab) and cetuximab in patients with operable head and neck squamous cell carcinoma

S. Temam[1*], J. Spicer[2], F. Farzaneh[3], J. C. Soria[4], D. Oppenheim[3], M. McGurk[5], A. Hollebecque[4], J. Sarini[6], K. Hussain[7], S. Soehrman Brossard[8], L. Manenti[9†], S. Evers[9], P. Delmar[8], L. Di Scala[8‡], C. Mancao[8§], F. Feuerhake[10,11], L. Andries[12], M. G. Ott[8¶,**], A. Passioukov[9**,††] & J. P. Delord[13**]

[1]Department of Head and Neck Surgical Oncology, Institut Gustave Roussy, Villejuif, France; [2]Division of Cancer Studies; [3]Department of Haematological Medicine, King's College London, London, UK; [4]DITEP (Drug Development Department), Gustave Roussy, Université Paris-Saclay, Villejuif, France; [5]Guy's & St Thomas' NHS Foundation Trust, London, UK; [6]Department of Surgery, Institut Claudius Regaud, Toulouse, France; [7]Head and Neck Surgery, King's College London, Guy's Hospital Campus, London, UK; [8]Roche Innovation Center Basel, Basel; [9]Roche Innovation Center Zurich, Schlieren, Switzerland; [10]Institute for Pathology, Hannover Medical School, Hannover; [11]Institute for Neuropathology, University Hospital Freiburg, Freiburg im Breisgau, Germany; [12]HistoGeneX, Antwerpen, Belgium; [13]Clinical Research Unit, Institut Claudius Regaud, Toulouse, France

Correspondence to: Dr Stéphane Temam, Department of Head & Neck Surgical Oncology, Institut Gustave Roussy, 114, rue Édouard-Vaillant, 94805 Villejuif Cedex, France. Tel: +33-1-42-11-44-46; E-mail: stephane.temam@gustaveroussy.fr

[†]Present address: Novartis, Basel, Switzerland.

[‡]Present address: Actelion, Allschwil, Switzerland.

§Present address: Genentech, Inc, Basel, Switzerland.

[¶]Present address: Pharma Development Basel, Roche, Switzerland.

[††]Present address: Pierre Fabre, Toulouse, France.

**These authors contributed equally to this work.

Background: In addition to inhibiting epidermal growth factor receptor (EGFR) signaling, anti-EGFR antibodies of the IgG_1 'subtype' can induce a complementary therapeutic effect through the induction of antibody-dependent cell-mediated cytotoxicity (ADCC). Glycoengineering of therapeutic antibodies increases the affinity for the Fc-gamma receptor, thereby enhancing ADCC.

Patients and methods: We investigated the changes in immune effector cells and EGFR pathway biomarkers in 44 patients with operable, advanced stage head and neck squamous cell carcinoma treated with two preoperative doses of either glycoengineered imgatuzumab (GA201; 700 or 1400 mg) or cetuximab (standard dosing) in a neoadjuvant setting with paired pre- and post-treatment tumor biopsies.

Results: Significant antitumor activity was observed with both antibodies after just two infusions. Metabolic responses were seen in 23 (59.0%) patients overall. One imgatuzumab-treated patient (700 mg) achieved a 'pathological' complete response. An immediate and sustained decrease in peripheral natural killer cells was consistently observed with the first imgatuzumab infusion but not with cetuximab. The functionality of the remaining peripheral natural killer cells was maintained. Similarly, a pronounced increase in circulating cytokines was seen following the first infusion of imgatuzumab but not cetuximab. Overall, tumor-infiltrating CD3+ cell counts increased following treatment with both antibodies. A significant increase from baseline in CD3+/perforin+ cytotoxic T cells occurred only in the 700-mg imgatuzumab group (median 95% increase, $P < 0.05$). The most prominent decrease of EGFR-expressing cells was recorded after treatment with imgatuzumab (700 mg, −34.6%; 1400 mg,

–41.8%). The post-treatment inflammatory tumor microenvironment was strongly related to baseline tumor-infiltrating immune cell density, and baseline levels of EGFR and pERK in tumor cells most strongly predicted therapeutic response.

Conclusions: These pharmacodynamic observations and relationship with efficacy are consistent with the proposed mode of action of imgatuzumab combining efficient EGFR pathway inhibition with ADCC-related immune antitumor effects.

Clinical trial registration number: NCT01046266 (ClinicalTrials.gov).

Key words: imgatuzumab, GA201, tumor-infiltrating lymphocytes, antibody-dependent cell cytotoxicity, squamous cell carcinoma of the head and neck, cetuximab

Introduction

Imgatuzumab (GA201) is a novel, recombinant, humanized, and glycoengineered IgG_1 monoclonal antibody (mAb) against the epidermal growth factor receptor (EGFR). Glycoengineering increases imgatuzumab's binding affinity for the Fcγ receptor IIIa (FcγRIIIa; CD16a) resulting in enhanced *in vitro* antibody-dependent cell-mediated cytotoxicity (ADCC) and superior preclinical anti-tumor efficacy with greater infiltration of ADCC-mediating immune cells into xenograft tumors versus cetuximab [1]. Imgatuzumab achieved objective responses in a phase I/II study of patients with EGFR-positive colorectal cancer, reduced circulating natural killer (NK) cells, and increased immune cell infiltration into imgatuzumab-associated skin rashes [2, 3].

A high density of tumor-infiltrating immune cells predicts disease-free and overall survival in different solid tumors [4–6], and both the number and distribution of these cells are likely to be important for mAbs that exert their therapeutic effect through immunological effector mechanisms. To better understand the contribution of immune cells to the efficacy of ADCC-enhancing anti-EGFR mAbs and to evaluate novel biomarkers for predicting response to immunomodulatory anti-EGFR therapy, we conducted an open-label study in patients with locally advanced resectable head and neck squamous cell carcinoma (HNSCC). This included an extensive biomarker program and innovative duplex immunohistochemistry markers for tumor immune cell subtyping.

Patients and methods

This prospective, multicenter trial randomized patients with operable HNSCC to receive two neoadjuvant infusions of imgatuzumab or cetuximab before surgical resection (supplementary Figure S1, available at *Annals of Oncology* online). The primary objective was to profile immune cell infiltration and activation in tumors following mAb therapy. Secondary objectives included assessment of immune cell and cytokine profiles in peripheral blood, biomarkers in tumor biopsies, anticancer activity using fluorodeoxyglucose-positron emission tomography (FDG-PET), and the safety of imgatuzumab. The study was conducted in accordance with the 'Declaration of Helsinki' and all patients provided written informed consent.

Eligible patients were adult with treatment-naive, advanced (stage T2–4) non-metastatic HNSCC considered resectable (see supplement for full inclusion/exclusion criteria). Patients were randomized (1 : 1 : 1) to imgatuzumab 700 mg, imgatuzumab 1400 mg, or standard-dose cetuximab (first dose: 400 mg/m^2; second dose: 250 mg/m^2). Patients received study drug on days 1 and 8 with surgical tumor excision planned for day 15. Further doses were allowed if surgical excision was delayed. All patients were pre-medicated with diphenhydramine (25–50 mg) and corticosteroid [hydrocortisone (200 mg) or equivalent]. Imgatuzumab was administered i.v. at 10 mg/hour (escalated to 300 mg/hour if well tolerated and started at 20 mg/hour for the second dose). Cetuximab was administered i.v. at 5 mg/mL over 120 minutes (60 minutes for the second dose).

Safety follow-up visits were conducted at 28 days and again 4 months after the last dose of study drug (or upon withdrawal from treatment).

FDG-PET was carried out as described previously [7] during screening and <3 days before surgery. All scans were interpreted centrally (IXICO Ltd, London).

Blood for peripheral immune cell assessments was collected at baseline and on days 1 and 8 (pre-dose, end-of-infusion, and 24 hours post-infusion). Circulating NK cells (CD3-/CD56+) were counted by flow cytometry (BD FACSCanto II/FACSDiva) and analyzed using FlowJo software. NK cell functionality was assessed by incubating peripheral blood mononuclear cells with EGFR-positive A431 target cells for 3 hours in the presence of imgatuzumab or cetuximab [3]. Using flow cytometry, CD16-dependent NK cell activation was calculated as the percentage of CD3–/CD56+ cells that became positive for CD107a. Details of antibodies used in flow cytometry and immunohistochemistry are in the supplementary material, available at *Annals of Oncology* online.

Fresh (not archival) paired tumor biopsies were taken at baseline and before surgery to ensure preanalytical equivalence. All attempts were made to use sequential tissue sections to ensure corresponding regions of tumor were analyzed in the separate immunohistochemistry analyses. The distribution of immune cells (CD3+, CD4+, CD8+, CD16+, CD56+, NKp46+, and CD68+) and EGFR pathway inhibition markers [EGFR and phosphorylated extracellular signal-regulated kinase (pERK)] were evaluated by immunohistochemistry, according to the standard methods. Chromogenic duplex marker staining was carried out to evaluate cytotoxic T cells, cytotoxic non T cells/NK cells, NK cells, CD16+ NK cells, and M1-type macrophages by combining perforin and major histocompatibility complex II (MHCII) staining with lineage markers such as CD3 and CD68. High-power fields (0.0156 mm^2) were randomly selected to represent the vital tumor mass with central and peripheral portions and the number of positive cells/mm^2 (mean of >15 high-power fields) was determined. For EGFR and pERK, sections were graded using H-Score, providing a number between 0 and 300 [8].

Changes in cytokine levels were assessed using blood obtained pre-dose, end-of-infusion, and 24 hours post-infusion (Luminex 50 cytokine panel).

Principal component analysis (PCA) examined the inter-relationships between baseline and on-treatment markers plus on-treatment markers and response. The strength of bivariate correlations was determined using Spearman rank correlation coefficients. Data from all cohorts were pooled for the baseline analysis but analyzed by treatment group for the on-treatment analysis. Changes in tumor biomarkers were evaluated using the Wilcoxon test.

Correlations between baseline intratumoral cytokines and baseline tumor immune-infiltration and the maximum standardized uptake value (SUV_{max}) were determined in assessable patients.

Results

Fifty-nine patients received neoadjuvant imgatuzumab or cetuximab (supplementary Figure S2, available at *Annals of Oncology*

Table 1. Treatment-emergent adverse events (safety population[a])

	Imgatuzumab 700 mg (*N* = 21)	Imgatuzumab 1400 mg (*N* = 20)	Cetuximab 400/250 mg (*N* = 18)[b]
Any AE	21 (100%)	20 (100%)	18 (100%)
AEs occurring in > 10% of patients in any arm			
Infusion-related reaction	16 (76%)	11 (55%)	3 (17%)
Folliculitis	7 (33%)	8 (40%)	2 (11%)
Rash	7 (33%)	5 (25%)	5 (28%)
Diarrhea	4 (19%)	2 (10%)	–
Nausea	3 (14%)	2 (10%)	–
Constipation	2 (10%)	3 (15%)	3 (17%)
Pyrexia	2 (10%)	3 (15%)	–
Anemia	1 (5%)	6 (30%)	3 (17%)
Any grade 3 or 4 AE	10 (48%)	14 (70%)	10 (56%)
Grade 3/4 AEs occurring in more than one patient in any arm			
Rash erythematous	2 (10%)	–	–
Infusion-related reaction	1 (5%)	3 (15%)	3 (17%)
Folliculitis	1 (5%)	4 (20%)	–
Rash	1 (5%)	2 (10%)	–
Dermatitis acneiform	–	2 (10%)	–
SAE[c]	5 (24%)	5 (25%)	5 (28%)
Deaths	–	–	1 (6%)[d]
Withdrawals due to AE	–	1 (5%)	3 (17%)

[a]The safety population was defined as the set of patients having received at least one infusion of study drug.
[b]Cetuximab given at 400 mg/m^2 for the first dose and 250 mg/m^2 for the second dose.
[c]No SAEs occurred in more than one patient in any treatment arm.
[d]One patient in the cetuximab group died (cardiac arrest, following Grade 4 respiratory distress and sepsis) which was assessed as unrelated to cetuximab.
AE, adverse event; SAE, serious adverse event.

online); most (54/59) received at least two infusions. The most common AEs were infusion-related reactions, folliculitis, rash, diarrhea, nausea, constipation, pyrexia, and anemia (Table 1). Grade 3 rash events occurred more frequently with the higher dose of imgatuzumab (40% versus 19% with the 700-mg dose). Grade 1/2 hypomagnesemia occurred in 5/21 (34.1%) and 9/20 (45.0%) patients in the imgatuzumab 700- and 1400-mg arms, respectively, and in 5/18 (27.8%) patients in the cetuximab arm. These hypomagnesemia events were not considered clinically significant and not reported as an AE. The lower incidence of rash events and hypomagnesemia, suggestive of a dose–event relationship, is consistent with previous data [2]. Four patients were withdrawn due to AEs: one from the imgatuzumab 1400-mg group and three from the cetuximab group (all grade 3 infusion-related reactions that resolved). One death occurred (a cardiac arrest in cetuximab-treated patient, considered unrelated to study treatment).

Forty-four patients received both planned antibody doses and had baseline and presurgery tissue biopsies and were thus evaluable for the primary endpoint (Table 2). An imbalance in baseline characteristics was observed. The 700-mg imgatuzumab group had smaller tumors, better performance status, and a higher proportion of females and oral tumors.

PET response data were available for 39/59 patients (Figure 1). Similar decreases in median SUV_{max} were observed for all treatments (–30.1%, –29.2%, and –31.7% for 700-mg imgatuzumab, 1400-mg imgatuzumab, and cetuximab, respectively). Decreases in total lesion glycolysis (TLG) [9] occurred in 10/14 (71.4%), 11/13 (84.6%), and 8/8 (100%) patients, respectively. Similarly, 8/15 (53.3%), 11/13 (84.6%), and 6/8 (75.0%) patients, respectively, had a decrease in PET volume. Eleven (64.7%), eight (57.1%), and four (50.0%) patients, respectively, achieved an EORTC partial metabolic response. One 700-mg imgatuzumab-treated patient achieved a pathological complete response.

Peripheral NK cell (CD3-/CD56+) counts decreased with imgatuzumab, but not with cetuximab (Figure 2A). The NK cells partially recovered and no further reduction occurred with subsequent infusions. Analysis of the CD16-dependent functional capacity of the remaining NK cells (CD107a assay; Figure 2B) showed that functionality was maintained after treatment with both antibodies.

The first imgatuzumab infusion was characterized by increased peripheral cytokine levels (supplementary Figure S3, available at *Annals of Oncology* online). A median change from pre-infusion to end-infusion of >10-fold was seen for MIP-1β, IP-10, interleukin (IL)-1RA, MCP1, MIG, and IL-15. Minimal or no changes in cytokine levels occurred after the second imgatuzumab infusion or after cetuximab administration.

Representative images of pretreatment and on-treatment hematoxylin and eosin stained sections are shown in supplementary

Table 2. Baseline characteristics of the 44 patients evaluable for the primary end point

	Imgatuzumab 700 mg (*N* = 15)	Imgatuzumab 1400 mg (*N* = 14)	Cetuximab 400/250 mg (*N* = 15)[a]
Age, years (range)	57 (45–68)	62 (52–69)	62 (42–74)
Gender (male/female)	**11/4**	14/0	13/2
ECOG-PS status (0/1/2)	**7/7/0**[b]	3/11/0	5/9/1
Number of infusions (2/3/4)	10/3/2	11/2/1	12/1/2
FcγRIII genotype (GG/TG/TT)	2/2/3	−/-/-	−/2/2
Stage (2/3/4)	1/3/10[b]	0/2/12	2/1/12
TN stage			
T1/T2/T3/T4/Tx	3/1/0/8/1[c]	0/4/1/9/0	0/4/1/10/0
N0/N1/N2	1/7/5[c]	6/0/8	6/0/9
Tumor location (O/P/L)	**13/2/0**	8/5/1	8/4/3
Tumor size (mm), median (range)	41 (22–70)	50 (22–150)	57 (22–100)
Tumor size, n (%)			
≤ 4 cm	**7 (46%)**	4 (29%)	5 (35%)
> 4 cm	8 (54%)	10 (71%)	9 (65%)[d]
HPV status (+/-/ND)[e]	2/7/3	4/3/4	3/5/7
Oncocarta Panel V1 mutations[f]	1	3	0
Immune cell infiltration and EGFR/pERK levels [median positive cells/mm^2 (range)][g]			
CD3 (T-lymphocyte)	**695 (83–1372)**	261 (68–1538)	261 (73–821)
CD4 (T-helper cell)	**349 (27–825)**	197 (58–868)	252 (68–812)
CD8 (T-cytotoxic cell)	**500 (24–892)**	158 (21–468)	141 (30–441)
CD16 (NK, FcγRIII)	**732 (299–1261)**	235 (43–464)	340 (94–948)
CD56 (NK cell)	5 (0–150)	7 (0–94)	17 (0–77)
NKp46 (NK cell)	34 (0–291)	38 (4–137)	17 (0–175)
CD68 (macrophage)	**501 (176–1222)**	177 (38–551)	248 (75–538)
EGFR [H-score]	184 (28–297)	178 (62–227)	174 (90–294)
pERK [H-score]	111 (23–195)	97 (44–183)	120 (29–187)
CD3+/PERF + (cytotoxic T cells)[h]	10.5 (0–48)	25 (1–390)	19 (0–304)
CD3-/PERF + (cytotoxic non T cells, NKs)[h]	10 (0–35)	7 (0–56)	12 (0–244)
CD3-/CD56 + (NK cells)[h]	**13 (0–42)**	**8 (0–26)**	2.5 (0–38)
CD16+/CD56 + (CD16+ NK cells)[h]	**12 (2–64)**	5 (0–11)	4 (0–32)
CD68+/MHCII + (M1 macrophages)[h]	158 (64–720)	99 (38–280)	160 (42–256)

[a]Cetuximab given at 400 mg/m^2 for the first dose and 250 mg/m^2 for the second dose.
[b]Data missing for one patient.
[c]Data missing for two patients.
[d]Tumor size not given for one patient.
[e]HPV status (genotypes 16, 18, 31, 33, 35, 39, 45, 51, 52, 56, 58, and 66) was assessed on DNA extracted from tumor material (pre-surgery and surgery material). HPV status not available for all patients; HPV cases were randomly distributed across arms with no apparent association with a change from baseline in SUV_{max}.
[f]700-mg imgatuzumab: one tumor had a *PIK3CA* E545K mutation, 1400-mg imgatuzumab: one tumor had a *MET* R970C mutation and two tumors had *PIK3CA* H1047R mutations. Only local PET SUV_{max} data were available for all four cases, with response ranging from −46.75 to −78.30%.
[g]Values represent the median number of positively stained cells per mm^2 tumor area (range). For EGFR and pERK, the values represent the median H-score (range). Multiple fields of view were examined. Bold text indicates values that were imbalanced between study arms.
[h]Duplex staining results were not available for all patients (imgatuzumab 700 mg: *N* = 8–13, imgatuzumab 1400 mg: *N* = 11–13, cetuximab 400/250 mg: *N* = 10–14).
CD, cluster of differentiation; ECOG-PS, Eastern Cooperative Oncology Group-performance status; EGFR, epidermal growth factor receptor; FcγR, Fcγ receptor; GG/TG/TT, guanine-guanine/thymine-guanine/thymine-thymine; HPV, human papilloma virus; mAb, monoclonal antibody; MHC, major histocompatibility complex; ND, not diagnostic; NK, natural killer; O/P/L, oral cavity/pharynx/larynx; PERF, perforin; pERK, phosphorylated extracellular signal-regulated kinase; PET, positron emission tomography; SUV_{max}, maximum standardized uptake value.

Figure S4, available at *Annals of Oncology* online, and immunohistochemistry sections in supplementary Figure S5, available at *Annals of Oncology* online. Baseline tumor-infiltrating immune cell densities were imbalanced between treatment arms, likely reflecting normal variability due to a heterogeneous inflammatory HNSCC tumor microenvironment. The 700-mg imgatuzumab group exhibited ≤3-fold higher baseline numbers of CD3+, CD4+, CD8+, CD16+, and CD68+ cells compared with the other

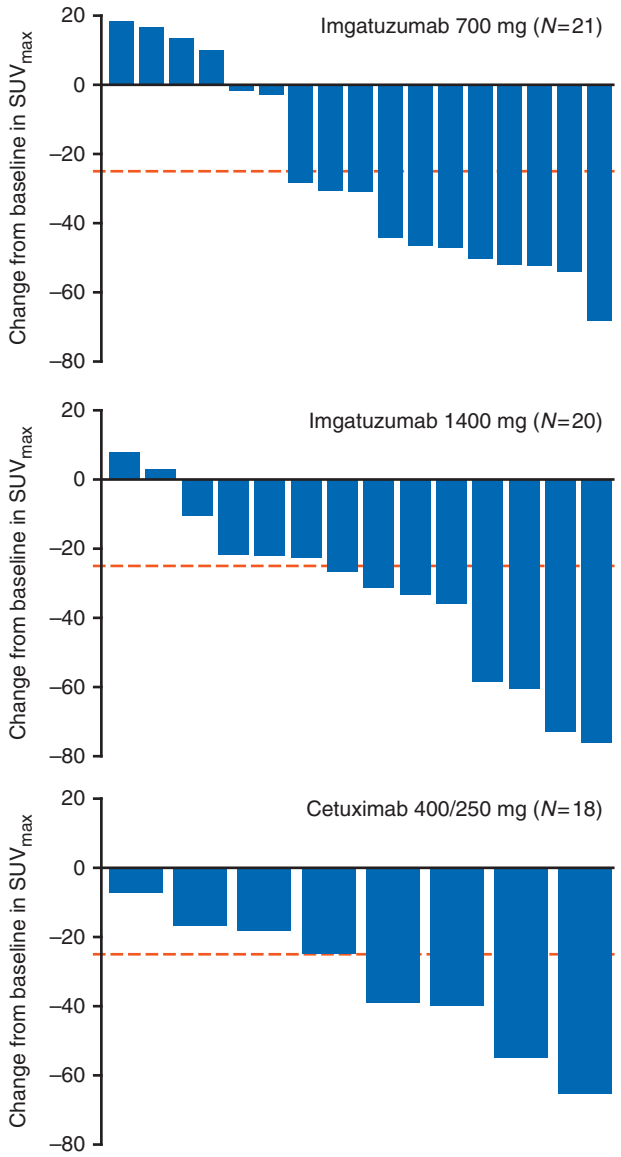

Figure 1. Waterfall plot showing the change in SUV_{max} in the head and neck region from baseline to post-mAb therapy per study arm for the safety population patients. The dotted line at –25% represents the EORTC recommended cut-off between the lower level of stable metabolic disease and the upper level of metabolic response. Centrally read PET scans were not available for four patients from the 700-mg imgatuzumab arm, six patients from the 1400-mg imgatuzumab arm, and 10 cetuximab patients. This was due to either missing baseline/post-mAb therapy PET scans, large differences in baseline and post-mAb therapy uptake times, or because the PET scans were done at non-qualified sites. EORTC, European Organization for Research and Treatment of Cancer; mAb, monoclonal antibody; PET, positron emission tomography; SUV_{max}, maximum standardized uptake value.

groups (Table 2). Despite this, levels of tumor-infiltrating immune cell subsets were generally well correlated at baseline (Table 3 and supplementary Figure S6, available at *Annals of Oncology* online). Correlations existed between T-cell markers (e.g. CD3/CD4 and CD3/CD8) and between T-cell markers and NK cell and macrophage markers (e.g. CD3, CD4, and CD8 with NKp46). PCA analysis showed that CD3/CD4/CD8/CD16/CD56/CD68/NKp46 were represented on the first principal component (PC1), cytoplasmic pERK on the second (PC2), and membrane EGFR on the third (PC3; supplementary Figure S7, available at *Annals of Oncology* online). Regression analysis indicated that higher baseline pERK and EGFR values predicted PET response better than immune markers (supplementary Figure S8, available at *Annals of Oncology* online). A clear differentiation in PET response was observed for patients with pERK H-score $\geq$73.38 versus $<$73.38 and a wide response range for patients with EGFR H-score $\geq$212.

Despite strong intrapatient variability, there was a consistent trend toward increasing on-treatment tumor immune-infiltration (especially T cells and NK cells) with both imgatuzumab and cetuximab (Figure 3 and supplementary Table S1, available at *Annals of Oncology* online). Cells expressing T-cell markers (CD3, CD4, and CD8), NK cell markers (CD56), and macrophages (CD68, CD68/MHCII) were generally more abundant on-treatment compared with pretreatment biopsies. There was no statistically significant difference between treatment arms regarding this common effect on the tumor immune infiltrate.

Tumor membrane EGFR expression decreased following treatment (Figure 3 and supplementary Table S1, available at *Annals of Oncology* online). Downregulation of EGFR was greatest with the 1400-mg imgatuzumab group (median change: –35% [700 mg]; –42% [1400 mg]; –21% [cetuximab]). Cells with the highest intensity EGFR staining (intensity 3) almost disappeared for both imgatuzumab groups (median change: –14% [700 mg] and –23% [1400 mg]). A decrease in cytoplasmic pERK levels was seen in 12/15, 10/14, and 12/15 patients in the 700-mg imgatuzumab, 1400-mg imgatuzumab, and cetuximab cohorts, respectively. The greatest decrease was observed with the 700-mg imgatuzumab group. A decrease of CD16, suggestive of CD16 engagement associated with ADCC, was only seen in the 700-mg imgatuzumab cohort.

Discussion

We report the results of a comprehensive biomarker program that investigated the additional contribution of modulating immune cell infiltration to the mode of action (MOA) of a glycoengineered and a conventional mAb. Both imgatuzumab and cetuximab induced intratumoral changes in T-cell, NK cell, and macrophage densities. The absence of clear differences in tumor immune infiltration patterns suggests that an increase in infiltrating T cells may reflect an ADCC-related process common to both therapies, or a more general response to EGFR pathway inhibition. An increase in CD8+ T-cell infiltration was recently described after treatment with the MEK inhibitor cobimetinib, in the absence of ADCC [10]. All patients received antihistamine and corticosteroid premedication, which might have affected immune effector cell recruitment. However, preclinical data with imgatuzumab indicate that ADCC potency is relatively unaffected by preincubation of effector cells with corticosteroids [11].

Distinct changes in FDG-PET SUV_{max} occurred after just two infusions with no differences between treatments. This can be mostly ascribed to the treatment effect on tumor cells, although induced inflammation might partially confound PET results as

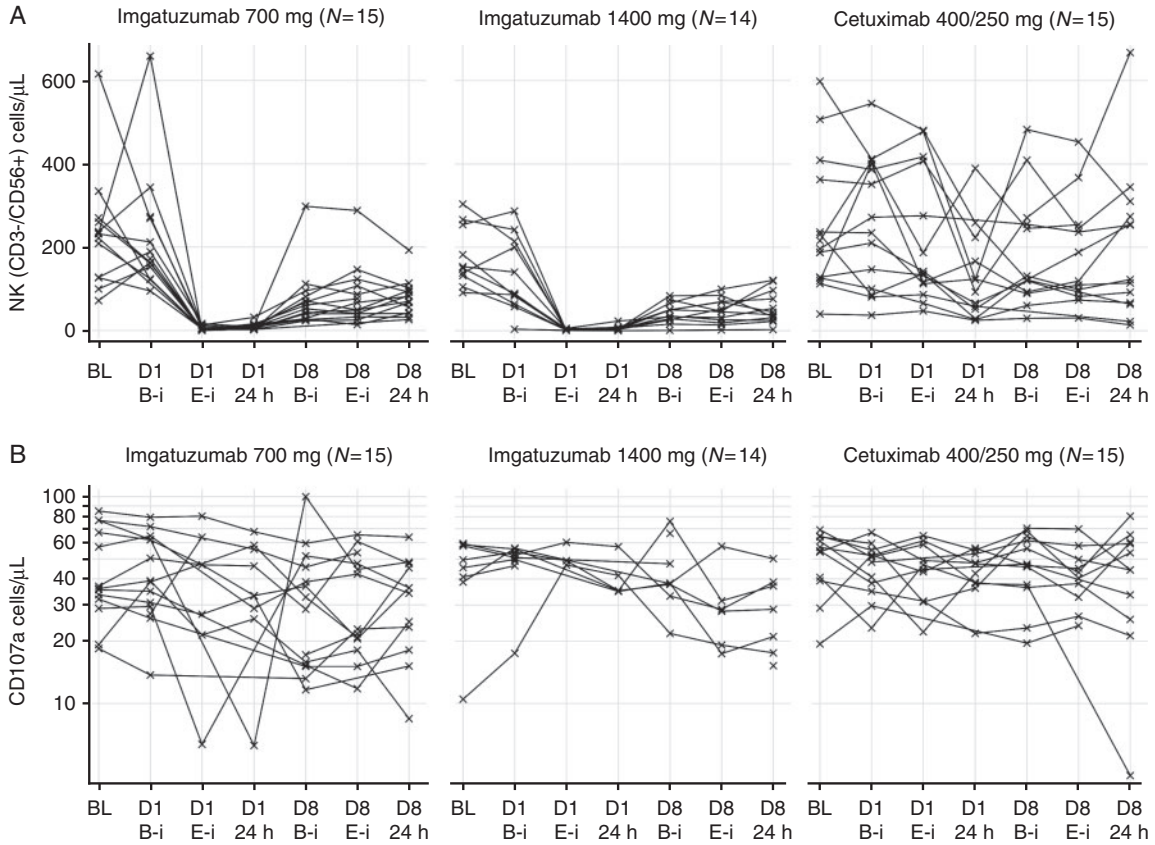

Figure 2. Kinetics of peripheral blood NK (CD3–/CD56+) cells (A) and CD16-dependent killing capacity of peripheral blood NK cells (B) following infusion of imgatuzumab or cetuximab. A dramatic decrease in the number of peripheral NK cells was seen with the first infusion of imgatuzumab (beginning as early as the end of the infusion) but not with cetuximab (A). NK cell numbers recovered to some extent by the time of the second infusion. The functional capacity of the remaining NK cells appeared relatively unchanged (B). BL, baseline; B-i, beginning of infusion; CD, cluster of differentiation; D1/8, day 1/8; E-i, end of infusion; NK, natural killer.

Table 3. Spearman r correlation coefficient between tumor immune cell markers and EGFR pathway markers at baseline (all assessable patients combined)

First marker	*r*-value for comparison with second marker								
	CD3	CD4	CD8	CD16	CD56	CD68	NKp46	EGFR M	pERK C
CD3	–	**0.67**	**0.85**	**0.63**	0.32	**0.64**	**0.59**	–0.11	0.12
CD4	**0.67**	–	**0.57**	**0.54**	**0.52**	0.45	**0.68**	–0.20	0.092
CD8	**0.85**	**0.57**	–	**0.53**	0.25	**0.59**	**0.59**	–0.18	0.14
CD16	**0.63**	**0.54**	**0.53**	–	0.19	**0.81**	0.45	0.00	0.25
CD56	0.32	**0.52**	0.25	0.19	–	0.27	0.43	–0.22	0.00
CD68	**0.64**	0.45	**0.59**	**0.81**	0.27	–	0.37	0.00	0.00
NKp46	**0.59**	**0.68**	**0.59**	0.45	0.43	0.37	–	–0.15	0.085
EGFR M	–0.11	–0.20	–0.18	0.00	–0.22	0.00	–0.15	–	–0.12
pERK C	0.12	0.092	0.14	0.25	0.00	0.00	0.085	–0.12	–

All *r*-values ≥0.50 are highlighted as bold text.
CD, cluster of differentiation; EGFR, epidermal growth factor receptor; NK, natural killer; pERK, phosphorylated extracellular signal-regulated kinase. Scatterplots for the individual biomarker combinations shown here can be found in supplementary Figure S6, available at *Annals of Oncology* online.

FDG can also accumulate within inflammatory cells [12]. It is unlikely that the observed PET effects were due to biopsy procedures which would be limited to a small part of the tumor. Other studies have shown that EGFR inhibitors generate an FDG-PET response that correlates with HNSCC proliferation [13].

The proposed MOA of the glycoengineered antibody was confirmed by the decrease in peripheral NK cells seen with imgatuzumab, consistent with previous phase I data [2]. Imgatuzumab might induce relocation or adhesion of NK cells to healthy tissues expressing low EGFR levels. Rituximab variants with high affinity for CD16 activate NK cells and upregulate cell adhesion molecules (e.g. CD54) to a higher degree than low-affinity variants [14, 15]. The high affinity of imgatuzumab for CD16 may cause the extravasation or endothelial adhesion of NK cells, notably through CD54 upregulation. The decrease in NK cells was not apparent with cetuximab, which has a lower affinity for CD16 [1]. This decrease in intratumoral CD16 with imgatuzumab (albeit only at the 700-mg dose) but not with cetuximab may also reflect the difference in CD16 affinity.

An increase in peripheral cytokines observed for the first imgatuzumab infusion that paralleled the acute decrease in NK cells, supports the proposed MOA. Increases of cytokines involved in the recruitment and activation of NK cells and T cells provides further evidence for CD16-mediated T-cell activation processes.

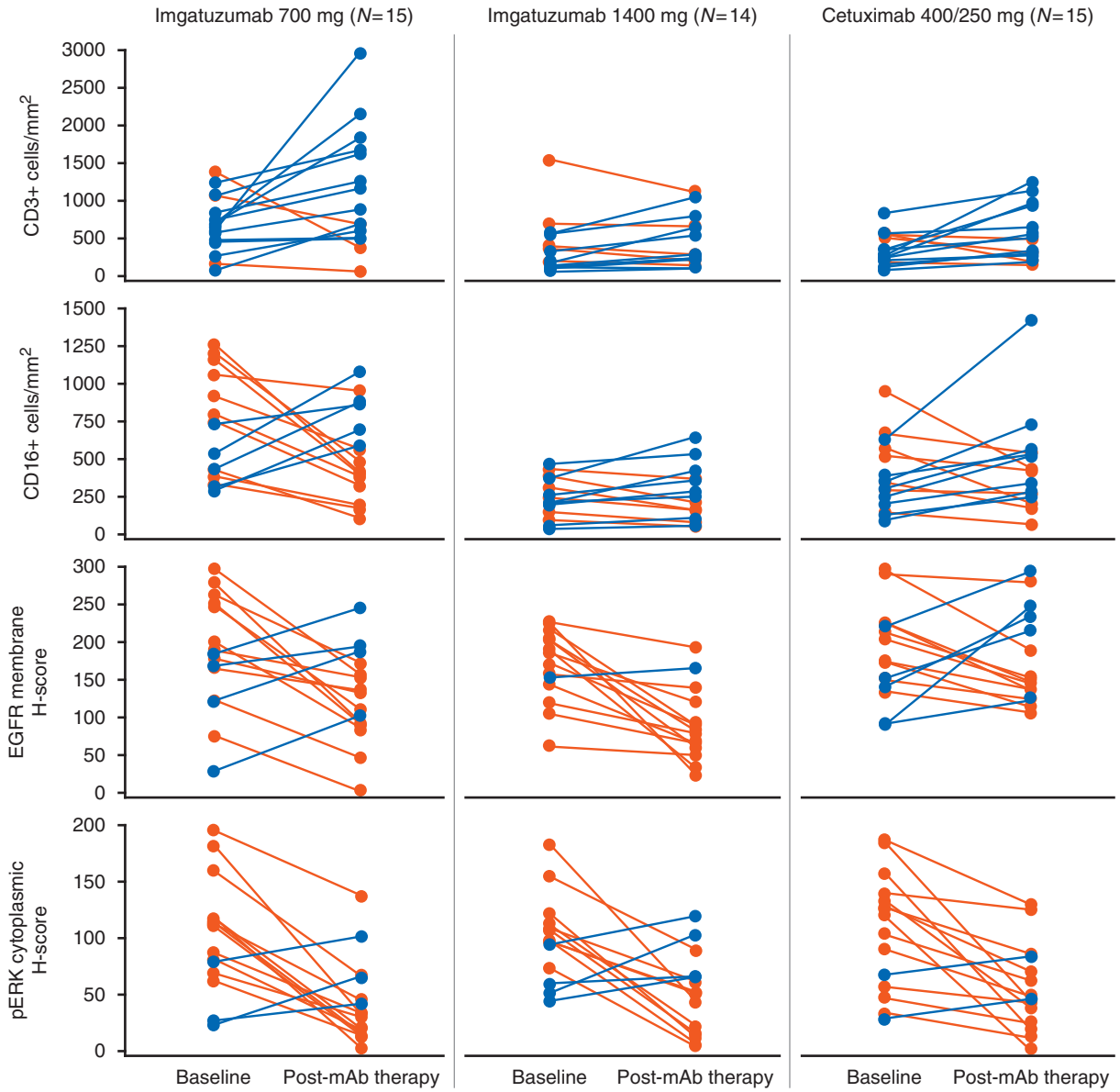

Figure 3. Immunohistochemistry data showing the change in immune infiltration and EGFR/pERK staining following treatment. Multiple fields of view were assessed for each tumor biopsy. Immunostaining was scored as the median number of positively stained cells per mm^2 for infiltrating CD3+ and CD16+ cells and using the H-score system [8] for EGFR and pERK immunohistochemistry. This scoring system combines the total percentage of cells staining with intensities of negative (0), weak (1), intermediate (2), and strong (3) to give a final value ranging from 0 to 300. Orange lines indicate patients in whom marker levels decreased after mAb treatment and blue lines indicate increases. Results show an on-treatment increase in immune infiltration with both antibodies and downregulation of EGFR and pERK. CD, cluster of differentiation; EGFR, epidermal growth factor receptor; mAb, monoclonal antibody; pERK, phosphorylated extracellular signal-regulated kinase.

Change in tumor immune cell infiltration, including an increase of CD3+/perforin+ cytotoxic T cells in the 700-mg imgatuzumab group, indicates specific effects on the immunocomposition of treated tumors. Baseline immune-infiltration was heterogeneous with highest median values in patients receiving 700-mg imgatuzumab who also exhibited the most pronounced on-treatment changes. This may indicate that, in this study, baseline immune infiltration was a more important determinant of immune response and efficacy than treatment or dose. Indeed, baseline immune-infiltration may be a useful efficacy biomarker for immune-competent compounds such as imgatuzumab. Strong baseline correlations existed between different markers of tumor-infiltrating cells, indicating that the samples differed in immune cell numbers rather than in immune cell subsets, whereas there was no correlation between infiltrating immune cell levels and EGFR pathway-related markers. With hindsight, the relationship between infiltrating immune cells and EGFR markers could have been investigated further with the inclusion of an erlotinib control treatment arm (showing EGFR inhibition in the absence of ADCC).

Imgatuzumab was as potent as cetuximab for EGFR pathway inhibition as evidenced by comparable EGFR/pERK

on-treatment changes, confirming that glycoengineering does not reduce anti-EGFR activity. Imgatuzumab toxicities were dose dependent, as expected for an EGFR inhibitor, and manageable. The mechanism responsible for clearance of tumor cells expressing high EGFR levels by imgatuzumab is most likely a combined MOA involving both EGFR downmodulation and increased ADCC-dependent killing.

In conclusion, these pharmacodynamic observations appear consistent with the conceptual MOA for both drugs. We found equal efficacy of imgatuzumab and cetuximab in terms of EGFR pathway inhibition, but showed several indicators for an additional ADCC-enhancing effect of imgatuzumab based on the on-treatment dynamics of peripheral immune cells and cytokines. However, enhanced ADCC activity did not translate into enhanced efficacy over cetuximab in a subsequent phase II trial: progression-free survival was similar for the second-line imgatuzumab plus FOLFIRI versus cetuximab plus FOLFIRI in *KRAS* wild-type metastatic colorectal cancer [16]. Imgatuzumab also failed to improve progression-free survival when added to cisplatin/premetrexed versus chemotherapy alone in metastatic non-squamous NSCLC [17]. Our innovative and comprehensive tumor biopsy protocol also revealed that the evaluation of immune cells in tumors with a heterogeneous inflammatory microenvironment such as HNSCC requires careful consideration of baseline conditions to accurately interpret post-treatment alterations in tumor-infiltrating cell densities.

Acknowledgements

The authors would like to thank the patients and their families for their participation in this study, the study management team, and the staff at the study sites. Special thanks also to Simon Hollingsworth (current affiliation AstraZeneca, UK) for a major contribution to the study design and biomarker program. All PET scans were interpreted by the independent specialist imaging company IXICO Ltd (London). Support for third-party writing assistance for this article, furnished by Jamie Ashman, PhD, was provided by Prism Ideas and funded by F Hoffmann-La Roche.

Funding

This work was supported by F Hoffmann-La Roche Ltd (no grant number applies). DO was awarded a fellowship from the Department of Health via the National Institute for Health Research (NIHR) Biomedical Research Centre award to Guy's & St Thomas' National Health Service (NHS) Foundation Trust in partnership with King's College London and King's College Hospital NHS Foundation Trust. The Experimental Cancer Medicine Centre at King's College London supported the translational medicine infrastructure in Farzin Farzaneh's laboratory.

Disclosure

CM, MGO, AP, SSB, PD, LDS, LM, and SE were employees of Roche at the time of the study and CM, LM, and SE hold stock/options in Roche. FFu was employee of Roche until 2012. In his present academic position, FFu received institutional research grants from Roche unrelated to this study. ST received travel support, honoraria, and remuneration from Roche for participating in meetings related to this study. JSp, FFa, DO, and KH received institutional research support/grants from Roche for this study and JPD and FFa received travel support from Roche. JPD received compensation for board membership and consultancy and institutional grants from Roche for other studies. JCS has received consultancy fees/honoraria from Roche for this and other studies. Author LA received funding from Roche for the immunohistochemical analyses reported in this manuscript. All remaining authors have declared no conflicts of interest.

References

1. Gerdes CA, Nicolini VG, Herter S et al. GA201 (RG7160): a novel, humanized, glycoengineered anti-EGFR antibody with enhanced ADCC and superior *in vivo* efficacy compared with cetuximab. Clin Can Res 2013; 19: 1126–1138.
2. Paz-Ares LG, Gomez-Roca C, Delord JP et al. Phase I pharmacokinetic and pharmacodynamic dose-escalation study of RG7160 (GA201), the first glycoengineered monoclonal antibody against the epidermal growth factor receptor, in patients with advanced solid tumors. J Clin Oncol 2011; 29: 3783–3790.
3. Delord JP, Tabernero J, Garcia-Carbonero R et al. Open-label, multicentre expansion cohort to evaluate imgatuzumab in pre-treated patients with KRAS-mutant advanced colorectal carcinoma. Eur J Cancer 2014; 50: 496–505.
4. Pagès F, Galon J, Dieu-Nosjean MC et al. Immune infiltration in human tumors: a prognostic factor that should not be ignored. Oncogene 2010; 29: 1093–1102.
5. Fridman WH, Pagès F, Sautès-Fridman C, Galon J. The immune contexture in human tumours: impact on clinical outcome. Nat Rev Cancer 2012; 12: 298–306.
6. Distel LV, Fickenscher R, Dietel K et al. Tumour infiltrating lymphocytes in squamous cell carcinoma of the oro- and hypopharynx: prognostic impact may depend on type of treatment and stage of disease. Oral Oncol 2009; 45: e167–e174.
7. Frings V, de Langen AJ, Smit EF et al. Repeatability of metabolically active volume measurements with ^{18}F-FDG and ^{18}F-FLT PET in non-small cell lung cancer. J Nucl Med 2010; 51: 1870–1877.
8. Pirker R, Pereira JR, von Pawel J et al. EGFR expression as a predictor of survival for first-line chemotherapy plus cetuximab in patients with advanced non-small-cell lung cancer: analysis of data from the phase 3 FLEX study. Lancet Oncol 2012; 13: 33–42.
9. Ryu IS, Kim JS, Roh JL et al. Prognostic value of preoperative metabolic tumor volume and total lesion glycolysis measured by 18F-FDG PET/CT in salivary gland carcinomas. J Nucl Med 2013; 54: 1032–1038.
10. Desai J, Hong YS, Kim JE et al. Efficacy and safety of cobimetinib (cobi) and atezolizumab (atezo) in an expanded phase 1b study of microsatellite-stable (MSS) metastatic colorectal cancer (mCRC). Annals Oncol 2016; 27: 470P.
11. Gonzalez-Nicolini V, Herter S, Lang S et al. Premedication and chemotherapy agents do not impair imgatuzumab (GA201)-mediated antibody-dependent cellular cytotoxicity and combination therapies enhance efficacy. Clin Cancer Res 2016; 22: 2453–2461.
12. Quon A, Fischbein NJ, McDougall IR et al. Clinical role of ^{18}F-FDG PET/CT in the management of squamous cell carcinoma of the head and neck and thyroid carcinoma. J Nucl Med 2007; 48: 58S–67S.
13. Vergez S, Delord JP, Thomas F et al. Preclinical and clinical evidence that Deoxy-2-[^{18}F]fluoro-D-glucose positron emission tomography with computed tomography is a reliable tool for the detection of early molecular responses to erlotinib in head and neck cancer. Clin Cancer Res 2010; 16: 4434–4445.

14. Bowles JA, Weiner GJ. CD16 polymorphisms and NK activation induced by monoclonal antibody-coated target cells. J Immunol Methods 2005; 304: 88–99.
15. Bowles JA, Wang SY, Link BK et al. Anti-CD20 monoclonal antibody with enhanced affinity for CD16 activates NK cells at lower concentrations and more effectively than rituximab. Blood 2006; 108: 2648–2654.
16. Bridgewater J, Cervantes A, Markman B et al. Efficacy and safety analysis of imgatuzumab (GA201), a novel dual-acting monoclonal antibody designed to enhance antibody-dependent cellular cytotoxicity, in combination with FOLFIRI compared to cetuximab plus FOLFIRI in second-line *KRAS* exon 2 wild type or with FOLFIRI alone in mutated metastatic colorectal cancer. J Clin Oncol 2015; 33: 669.
17. Paz-Ares L, Calvo E, Kalinka-Warzocha E et al. GAIN-(L): Efficacy, safety and biomarker analysis of RG7160 (GA201), a novel dual-acting monoclonal antibody designed to enhance antibody-dependent cellular cytotoxicity, in combination with 1st line cisplatin and pemetrexed in metastatic non-squamous NSCLC. Ann Oncol 2013; 24: 3415.